Supplementary Information (SI) for Lab on a Chip.
This journal is © The Royal Society of Chemistry 2026

Rapid Desiccation and On-disc Rehydration of Extracellular Vesicles for Non-cryogenic Preservation

Hyun-Kyung Woo[1,2], Sangjin Seo[1,2], Advitiya Mahajan[3], Seoyoung Lee[1,2], Seoyoon Bae[1,2], Jeremy M. Quintana[1,2], Changhyun Kim[4], Alptekin Aksan[3]*, Hakho Lee[1,2]*

[1] Center for Systems Biology, Massachusetts General Hospital Research Institute, Boston, MA, USA
[2] Department of Radiology, Massachusetts General Hospital, Harvard Medical School, Boston, MA, USA
[3] Biostabilization Laboratory, Department of Mechanical Engineering, University of Minnesota, Minneapolis, MN 55455, USA
[4] Department of Surgery, Chonnam National University Hwasun Hospital, Chonnam National University Medical School, Hwasun, Korea

KEYWORDS: extracellular vesicles (EVs), non-cryogenic preservation, ambient storage, centrifugal microfluidic device, desiccation

*Corresponding authors:

Alptekin Aksan, PhD
Department of Mechanical Engineering
University of Minnesota
Minneapolis, MN, 55455
aaksan@umn.edu

Hakho Lee, PhD
Center for Systems Biology
Massachusetts General Hospital
185 Cambridge St, CPZN 5206
Boston, MA, 02114
hlee@mgh.harvard.edu

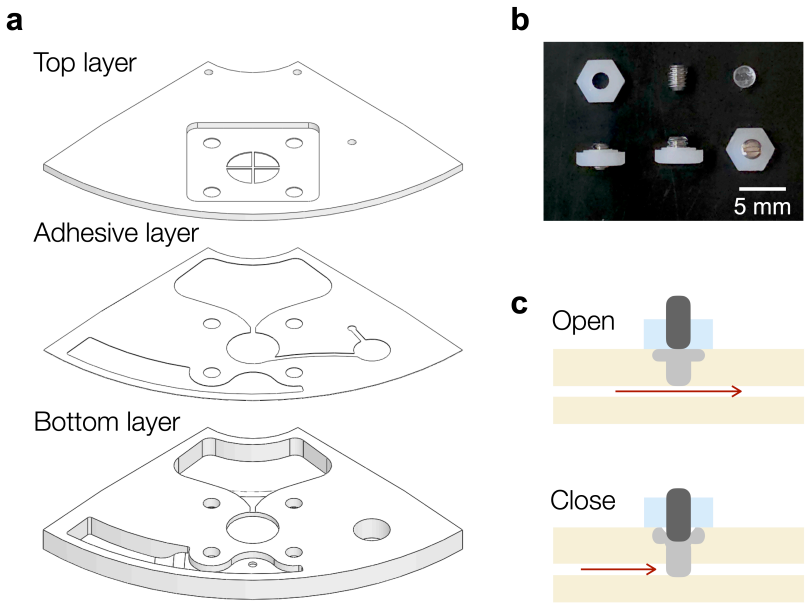

Figure S1. Components of the AridEx device. (a) The device is composed of three main layers: a top layer and a bottom layer made of PMMA, and an adhesion layer of pressure-sensitive double-sided tape. These layers are laminated to form a sealed chamber for sample processing. **(b)** Photographs of the valve components and assembly. (Top) Individual components (from left to right): nylon nut, threaded set screw, and elastic diaphragm. (Bottom) Side and top views of the assembled valve. **(c)** Operational states of the valve: Open state (top) and closed state (bottom). The valve is reversibly actuated by rotation of the set screw.

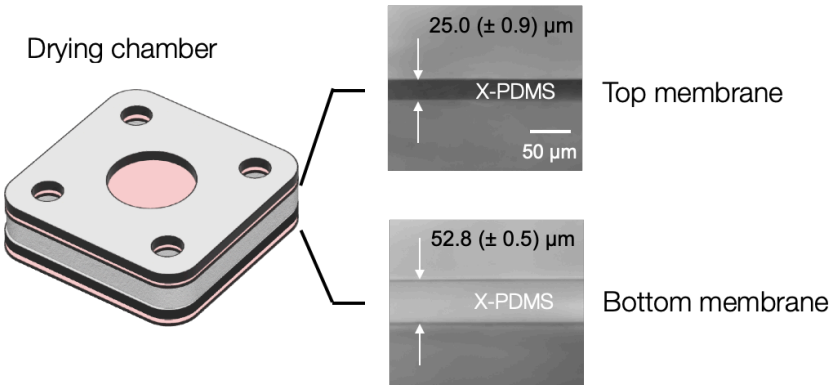

Figure S2. Drying chamber with X-PDMS membranes. The drying chamber was enclosed by two gas-permeable X-PDMS membranes: a top membrane with a thickness of 25.0 μm and a bottom membrane with a thickness of 52.8 μm.

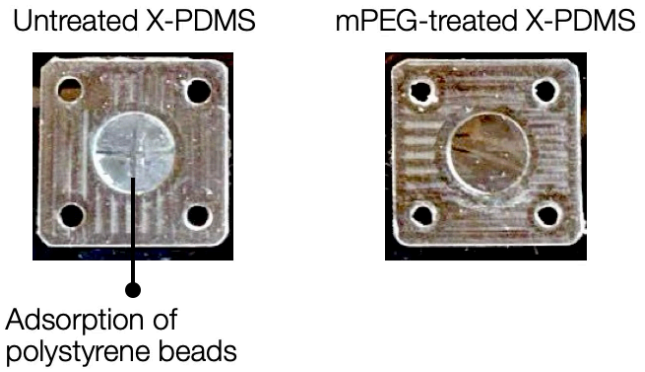

Figure S3. Comparison of sample adsorption in the desiccation chamber. A control AridEx device incorporated a desiccation chamber with unmodified X-PDMS membranes, while a comparative device had X-PDMS membranes modified with mPEG. Samples containing polystyrene microbeads (5 μm in diameter) were introduced into both devices, which subsequently underwent vacuum drying, sample rehydration, and bead transfer to a collection chamber. Following these processes, the desiccation chambers were imaged for residual bead retention. In the control device, significant bead adhesion was observed on the unmodified X-PDMS membranes. Conversely, the device incorporating mPEG-modified X-PDMS membranes showed minimal bead retention.

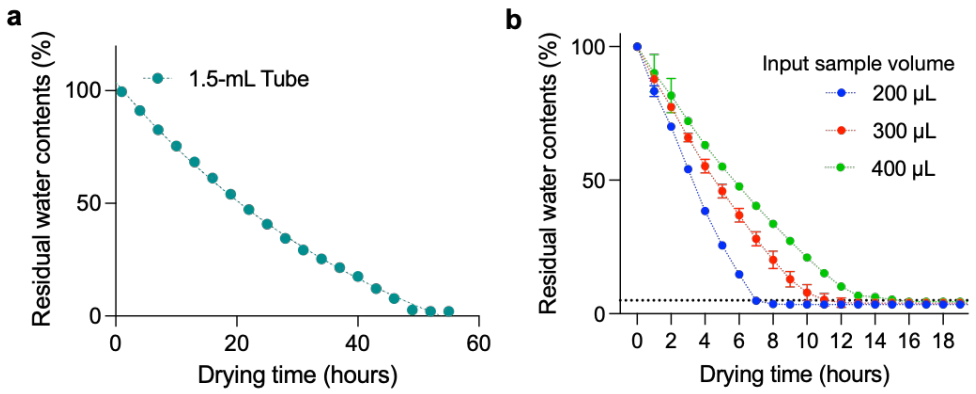

Figure S4. Sample drying kinetics with xeroprotectant. (a) Aqueous samples (200 μL) were dispensed into standard 1.5 mL tubes pre-loaded with a xeroprotectant. These tubes were subsequently vacuum-dried. The total mass of each tube was measured hourly to quantify the extent of sample evaporation. Complete dehydration was achieved after approximately 50 hours of vacuum drying. Data are presented as mean ± s.d. from technical duplicates. **(b)** AridEx dehydration kinetics as a function of sample buffer volume. Increasing the buffer volume proportionally extends the time required to reach the target residual moisture level (<5%, dotted line). Data are presented as mean ± s.d. from technical duplicates.

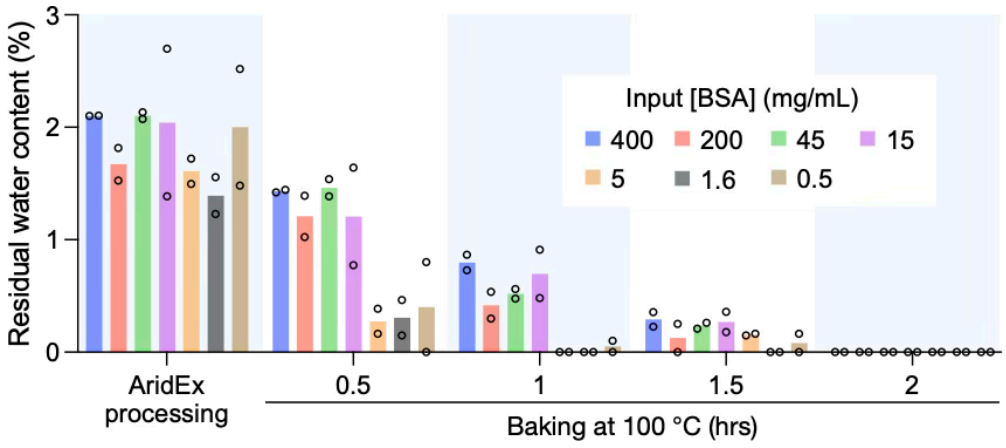

Figure S5. Influence of protein concentration on AridEx drying performance. Samples with varying concentrations of bovine serum albumin (BSA) were used to evaluate the effect of protein concentration on drying efficiency. The residual mass after AridEx drying was consistently less than 3% of the initial water content across all tested concentrations. Upon baking at 100 °C, the residual mass became negligible, indicating that moisture was the primary cause. The bars represent the average values from technical duplicates.

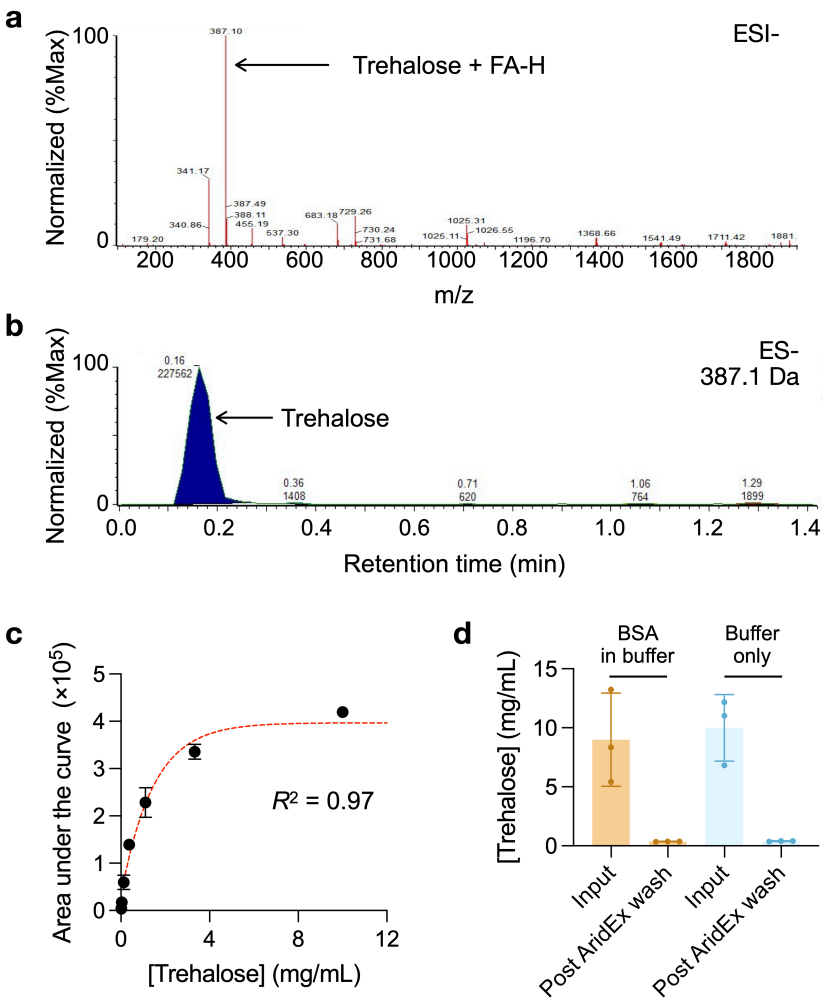

Figure S6. Quantification of residual trehalose following AridEx washing. (a) Liquid chromatography-mass spectrometry (LC-MS). The mass spectrum of the chromatographic peak at 0.15 min, acquired in negative electrospray ionization (ESI-) mode, confirmed the presence of trehalose by the characteristic formate adduct ion (m/z 387.1 [M+FA–H]). FA, formic acid. **(b)** Representative extracted ion chromatogram of the m/z 387.1 signal. The peak at 0.15 min was integrated for quantification. **(c)** Calibration curve relating trehalose concentration to integrated peak area. **(d)** Calculated residual trehalose concentrations in AridEx-washed samples, demonstrating levels below 0.5 mg/mL (<5% of the initial concentration). Data are displayed as mean ± s.d. from technical triplicates.

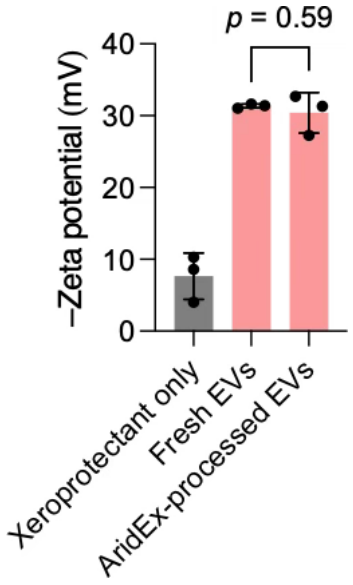

Figure S7. Colloidal stability of AridEx-stored EVs. Zeta potential measurements showed no significant difference ($p = 0.59$; unpaired two-sided *t*-test) between fresh (31.4 ± 0.3 mV) and AridEx-stored EVs (30.4 ± 2.8 mV). Data are displayed as mean ± s.d. from technical triplicates.

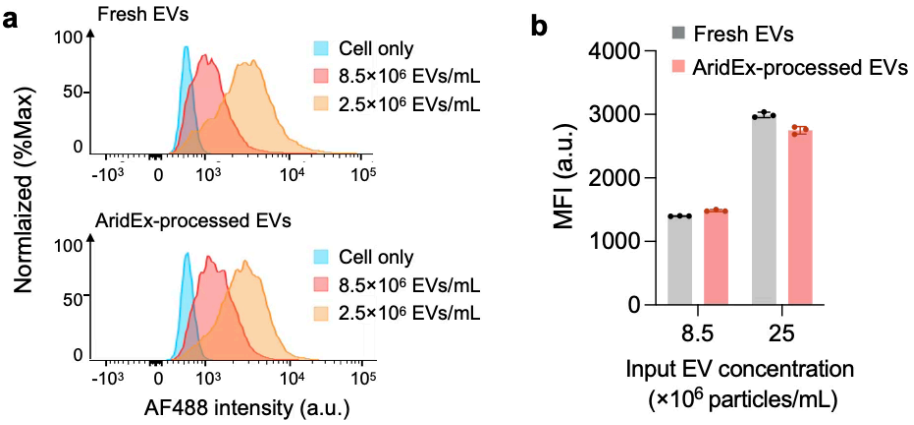

Figure S8. Cellular uptake of AridEx-stored EVs. (a) Representative flow cytometry histograms of HEK293 cells incubated for 24 h with AF488-labeled fresh or AridEx-stored EVs. **(b)** Quantification of median fluorescence intensity (MFI) at two EV doses. Cellular uptake was comparable between fresh and AridEx-stored EVs. The bars represent the average values from technical triplicates.

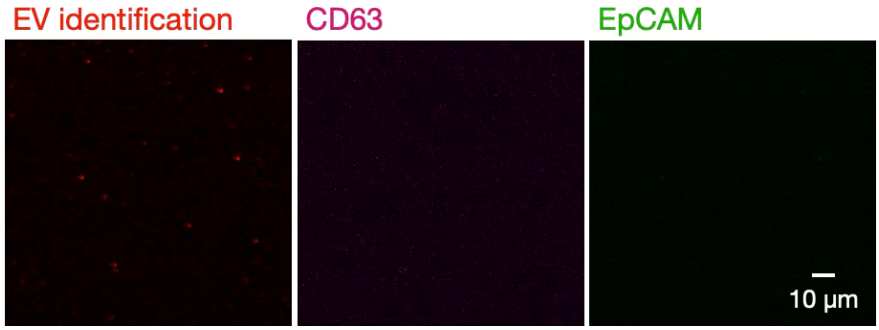

Figure S9. Single particle imaging of EVs stored in a buffer. SW620-derived EVs were stored in PBS buffer at 22 °C for 6 months. Following this storage period, samples were fluorescently labeled for EV identification (amine-reactive dye, AF555) and immunolabeled for CD63 (AF647) and EpCAM (AF488). The particle count was low in the EV-identification channel, indicating EV degradation. Furthermore, no signal was detected in the CD63 or EpCAM channels.

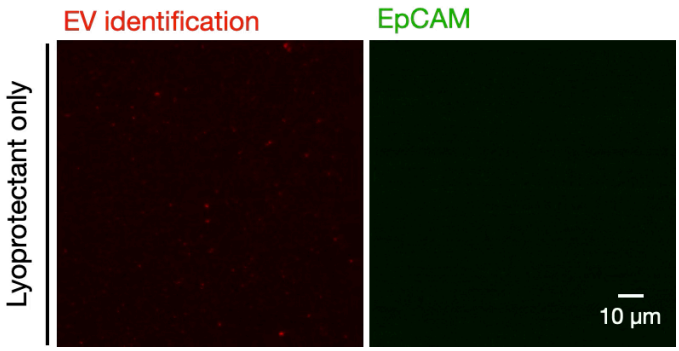

Figure S10. Single particle imaging of xeroprotectant-only control. Single-particle imaging was conducted on xeroprotectant-only control samples, following the identical protocol employed for EV-containing samples. Samples were labeled with an amine-reactive dye (for EV identification) and subjected to immunostaining for EpCAM (AF488). No discrete particles were observed in either detection channel, indicating that the xeroprotectant alone does not contribute to false-positive signals in single-extracellular EV imaging.

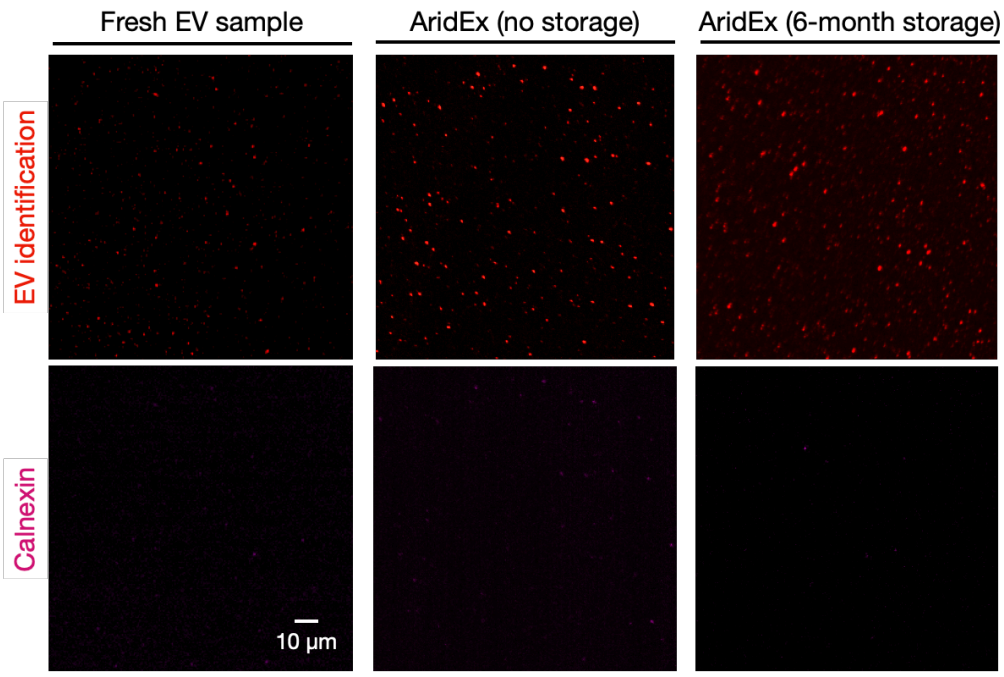

Figure S11. Evaluation of an EV-negative marker. Calnexin expression was assessed as a negative marker for EVs. SW620-derived EV samples were analyzed under three conditions: fresh, AridEx-processed without storage, and AridEx-processed with 6 months of storage. These samples were subjected to dual fluorescent labeling for EV identification and immunolabeling for calnexin. No detectable calnexin signals were observed under these tested conditions.

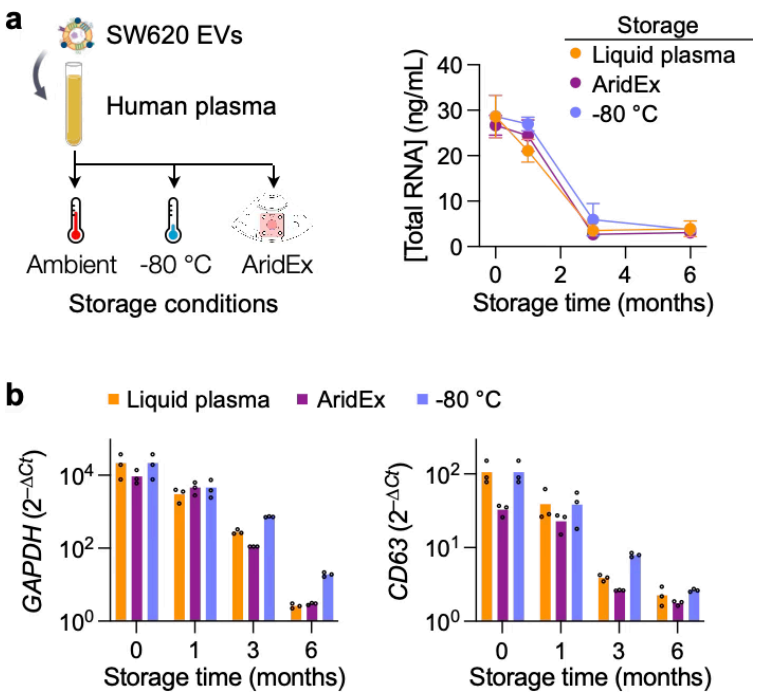

Figure S12. EV RNA analysis in preserved plasma samples. (a) EVs from SW620 cells were spiked into human plasma. Samples were divided into three storage groups: ambient conditions (liquid plasma), low-temperature freezing (-80 °C), and AridEx storage at ambient conditions. At 0, 1, 3, and 6 months of storage, total RNA was quantified from EVs preserved under each storage condition. The RNA amount remained stable for one month and declined across all three storage conditions. Data are displayed as mean ± s.d. from technical triplicates. **(b)** RT-qPCR analysis of EV mRNA targets (*GAPDH* and *CD63*) showed similar degradation trends across storage groups. *Ct*, cycle threshold value. Data are displayed as mean ± s.d. from technical triplicates.

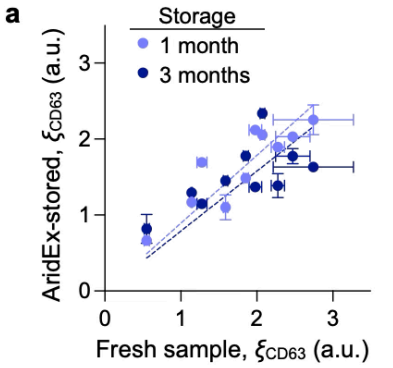

Pearson's *r*

CD63	Fresh	1-month AridEx	3-month AridEx
Fresh	1	0.88	0.67
1-month AridEx		1.00	0.60
3-month AridEx			1

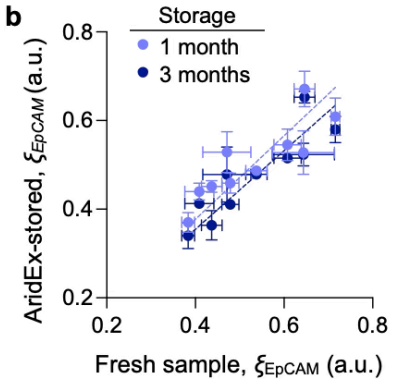

Pearson's *r*

EpCAM	Fresh	1-month AridEx	3-month AridEx
Fresh	1	0.92	0.94
1-month AridEx		1.00	0.97
3-month AridEx			1

Figure S13. Comparison of marker expression between fresh and AridEx-stored clinical plasma samples. Fresh plasma samples from CRC patients ($n = 5$) and non-cancer donors ($n = 5$) were biotinylated and analyzed for total EV loading (via fluorescent streptavidin staining) and the expression of CD63 and EpCAM (via immunostaining). Aliquots of unstained fresh samples were AridEx-stored for 1 and 3 months, and subjected to the same analytical procedures. The levels of CD63 (ξ_{CD63}) and EpCAM (ξ_{EpCAM}) were determined by scaling the marker expression against EV loading. **(a)** CD63 levels were compared between AridEx-stored and fresh plasma samples. Both 1-month and 3-month AridEx-stored samples showed a good correlation with fresh samples. The Pearson's correlation coefficient (r) values were 0.88 (1-month AridEx vs. fresh sample) and 0.67 (3-month AridEx vs. fresh sample). **(b)** Similarly, EpCAM expression demonstrated a good correlation between AridEx-stored and fresh samples, with $r = 0.92$ (1-month AridEx vs. fresh sample) and 0.94 (3-month AridEx vs. fresh sample). Data are displayed as mean ± s.d. from technical duplicates.

Table S1. AridEx operation parameters.

Step	No.	Speed (rpm)	Time (sec)	Operation
EV loading	1	1200	60	EV transfer to filter chamber
Mixing	2	5 rocking modes†	300	EV mixing with NCP
Rehydration	3	5 rocking modes†	300	Rehydration with buffer
	4	1200	1800	Wash I
	5	5 rocking modes†	300	Rehydration with buffer
	6	1200	1800	Wash II
EV collection	7	1200	30	EV transfer to collection chamber
Total time (min)			76.5	

†Rocking mode: ±120° oscillation/sec for 30 sec, followed by 1200 rpm rotation for 30 sec. All procedures are conducted at 20°C.

Table S2. List of antibodies used in the current work.

	Marker	Vendor	Host
Primary	CD63	Ancell (215-820)	Mouse IgG1
	EpCAM	Abcam (ab187372)	Mouse IgG1
Isotype	Mouse IgG1	Bioxcell (BE0083)	Mouse
Fluorescent label	Mouse IgG (H&L) AlexaFluor 488	Thermofisher scientific (A11001)	
	StAv PE	Biolegend (405203)	

Table S3. Primer sequences used for RT-PCR.

Primer	Sequence (5’ → 3’)
GAPDH forward	GTC TCC TCT GAC TTC AAC AGC G
GAPDH reverse	ACC ACC CTG TTG CTG TAG CCA A
CD63 forward	CAA CCA CAC TGC TTC GAT CCT G
CD63 reverse	GAC TCG GTT CTT CGA CAT GGA AG